International Immunopharmacology 76 (2019) 105887

Contents lists available at ScienceDirect

International Immunopharmacology

journal homepage: www.elsevier.com/locate/intimp

MicroRNA-23b alleviates neuroinflammation and brain injury in intracerebral hemorrhage by targeting inositol polyphosphate multikinase

Liuting Hu[a], Heyu Zhang[d], Bingyang Wang[a], Qiang Ao[b], Jing Shi[c], Zhiyi He[a,*]

[a] Department of Neurology, The First Affiliated Hospital of China Medical University, Shenyang, 110000,People's Republic of China
[b] Department of Tissue Engineering, China Medical University, Shenyang 110122, People's Republic of China
[c] Department of Neurology, Dandong Central Hospital, Dandong 118002,People's Republic of China
[d] Dapartment of Neurology, The First Affiliated Hospital Sun Yat-sen University,Guangzhou 510080,People's Republic of China

ARTICLE INFO

Keywords:
Intracerebral hemorrhage
Neuroinflammation
MicroRNA-23b
Inositol polyphosphate multikinase
Autophagy
Neuroprotection

ABSTRACT

Neuroinflammation plays a critical role in the pathogenesis of intracerebral hemorrhage (ICH), contributing to detrimental brain injury and neurological function deficits. MicroRNA-23b (miR-23b) exerts anti-inflammatory effects in many diseases and is downregulated in patients with ICH. This study aimed to evaluate the involvement of miR-23b in ICH models *in vivo* and *in vitro*, using basal ganglia injection of collagenase type VII in rats and hemin stimulation for cells, respectively. Exogenous overexpression of miR-23b by transfection with lentivirus-miR-23b (LV-miR-23b) or miR-23b mimics was evaluated by RT-qPCR. In this study, we found miR-23b was downregulated in the ICH models and its overexpression effectively alleviated neurological deficits, brain edema, hematoma area, and neuronal apoptosis in ICH rats. Western blotting for neuroinflammation markers and immunofluorescence staining for microglial activation demonstrated that miR-23b could alleviate neuroinflammation in ICH *in vivo*. We also performed an *in vitro* mechanism study using BV2 microglial cells and HT22 neuronal cell lines to explore how miR-23b modulates neuroinflammation and neuronal protection after ICH. We found that miR-23b significantly decreased hemin-stimulated inflammation response in BV2 cells and attenuated co-cultured HT22 neuronal cell death. Additionally, we verified that miR-23b suppressed inflammation in BV2 cells by targeting inositol polyphosphate multikinase (IPMK) and that autophagy regulation through the Akt/mTOR pathway was involved in miR-23b-regulated inflammation after ICH. Our study illustrated that miR-23b played a protective role in ICH through inhibiting neuroinflammation by targeting IPMK; this mechanism may be related to the regulation of the Akt/mTOR autophagy pathway, making it a potential target for ICH treatment.

1. Introduction

Intracerebral hemorrhage (ICH), a stroke subtype, is a serious public health issue with high mortality and morbidity rates [1]. ICH injury can be divided into primary and secondary injury. The former is caused by mechanical damage following initial bleeding, while the latter is caused by diverse mechanisms including inflammation, oxidative stress, mitochondrial dysfunction, and neuronal death [2–5]. Although the pathophysiological mechanisms of ICH have been extensively studied, effective treatments for ICH remain limited and need to be further explored.

Increasing evidence suggests that neuroinflammation, including activation of microglia, release of inflammatory cytokines, microglia polarization, and infiltration of polymorphonuclear neutrophils, plays an important role in ICH pathogenesis [6–9]. Previous studies have shown that inhibition of neuroinflammation can effectively ameliorate ICH-induced neuronal cell death and alleviate ICH-induced injury, making it a therapeutic strategy for ICH [10–14]. Recently, studies have demonstrated that autophagy, a process of cell self-eating for energy recycling, is implicated in the process of ICH [15,16], and inhibition of autophagy can perform a protective role in ICH, which can relieve neuroinflammation and neuronal death [17–19]. However, molecular mechanisms underlying the regulation between autophagy and neuroinflammation of ICH remain to be identified.

MicroRNAs are non-coding RNAs(18–22 nucleotides) that regulate diverse fundamental biological and pathological processes by post-transcriptionally regulating target mRNAs [20]. There is increasing evidence that miRNAs play an important role in ICH. For instance,

* Corresponding author at: Department of Neurology, The First Affiliated Hospital of China Medical University, 155N, Nanjing Street, Heping District, Shenyang 110000, People's Republic of China.
E-mail address: hezhiyi0301@sina.com (Z. He).

https://doi.org/10.1016/j.intimp.2019.105887
Received 6 June 2019; Received in revised form 21 August 2019; Accepted 5 September 2019
Available online 16 September 2019
1567-5769/

microRNA-367 attenuates inflammation and brain injury in ICH by targeting interleukin-1 receptor-associated kinase 4 (IRAK4) [21], and microRNA-132 alleviates neurobehavioral and neuropathological changes of ICH [22]. MicroRNA-23b (miR-23b) is located on human chromosome 9.Previous studies on miR-23b have mostly focused on its effects on cancers, such as lung, prostate, and gastric cancers [23–25], but its role in neuroscience is currently limited. Recently, several researchers have found that miR-23b was downregulated in experimental autoimmune encephalomyelitis (EAE) and played an anti-inflammatory role in CNS inflammation, alleviating the severity of EAE [26]. Furthermore, our previous miRNA array study showed that miR-23b was down-regulated in ICH patients compared with the levels in normal controls [27], but whether miR-23b down-regulation is involved in the pathogenesis of ICH remains unclear.

In this study, we aimed to investigate the role and the underlying mechanisms of miR-23b in ICH, using a collagenase type VII-induced rat ICH model and a hemin-stimulated cell model.

2. Materials and methods

2.1. Animals

Adult male Wistar rats weighing 250–280 g were provided by Liaoning Changsheng Biotechnology Co. Ltd. (China). All experimental protocols involving animals were approved by the Animal Care and Use Committee of China Medical University (2012-38-1) and complied with the ARRIVE guidelines. All animals were housed in separate cages, controlled temperature and light/dark cycles were maintained, and animals had free access to food and water.

2.2. Experimental groups in vivo

To examine miR-23b expression after intracerebral hemorrhage, 38 rats were randomly divided into two groups: sham group (n = 18) and ICH group (n = 18/20, number of successful models/total number of ICH models, same below). Next, 18 rats in each group were randomly divided into three sub-groups. Six rats were decapitated on day 1, six more on day 3, and the remaining six on day 5, and brain samples were collected for biochemical testing.

To explore the effects of miR-23b on ICH, 102 rats were randomly assigned to four groups: sham (n = 24), ICH (n = 24/27), ICH + lentivirus-miRNA negative control (LV-miR-NC; n = 24/26) and ICH + lentivirus-miR-23b (LV-miR-23b; n = 24/25). Next, 24 rats in each group were randomly divided into four sub-groups. Six rats were decapitated on day 3 after ICH, to analyze the brain water content; six were perfused with fixative for histological analysis on day 3 after ICH, six more were decapitated on day 3 after ICH for biochemical analysis of the perihematomal region, and six were used for assessments of neurological function deficits until the fifth day after ICH.

2.3. Intracerebroventricular injection of lentivirus and establishment of ICH model in rats

As previously described [28], the rats were anesthetized with sodium pentobarbital and fixed in a stereotaxic frame. A cranial burr hole (1 mm in diameter) was made with a dental drill and 5 μl LV-miR-23b or LV-miR-NC (10^9 transfection unit/ml), constructed by the GeneChem Company (China), was slowly injected into the right lateral ventricle (stereotaxic coordinates: 1.5 mm posterior, 1.8 mm right lateral to the bregma, and 3.5 mm ventral to the skull), at a rate of 0.5 μl/min using a microinjection pump. Two weeks later, the ICH model was induced in accordance with the study of Rosenberg et al. [29], and 0.5 U of collagenase VII (Sigma Aldrich, USA) was infused into the right caudate nucleus (stereotaxic coordinates: 1.0 mm posterior, 3.0 mm right lateral to the bregma, and 6.0 mm ventral to the skull), at a rate of 0.4 μl/min through another 1 mm burr hole, while the sham group underwent the same surgical procedures without intracerebral injection. After the rats recovered from anesthesia, they were placed in their home cages and had free access to food and water.

2.4. Neurological deficits tests and measurement of brain water content

Neurological deficits tests, including the corner tests and limb placement tests, were conducted on days 1,3 and 5 after ICH as previously described [30]. All tests were conducted by an investigator who was blinded to the grouping of the animals. The wet weight of the ipsilateral cerebral hemisphere was obtained using an electronic balance, and the dry weight was obtained after the brain was dried at 100 °C for 24 h. Water content was calculated as (wet weight-dry weight)/wet weight x100%.

2.5. Hematoxylin and eosin (H&E) staining and immunofluorescence staining

Three days after ICH induction, rats were transcardially perfused with saline, followed by 4% paraformaldehyde; the rat brains were isolated and postfixed overnight, and soaked in 15% and 30% sucrose for one day each at 4 °C. The brains were then frozen and 8 μm-thick frozen brain sections were collected.

H&E staining was conducted using an H&E staining kit following the manufacturer's instructions (Solarbio, China). Immunofluorescence staining of ionized calcium binding adaptor molecule 1 (Iba1) for detecting microglia activation and neuronal nuclei (NeuN) for neurons was also conducted. After rewarming at room temperature, the slides were soaked in 0.3% Triton X-100 for 10 min and blocked with 4% bovine serum albumin for 1 h at 37 °C, followed by subsequent incubation with mouse anti-Iba1 (1:200, Abcam, USA) or mouse anti-NeuN (1:200, Abcam, USA) overnight at 4 °C. After three thorough PBS washes, Alexa 594 secondary antibodies (1:500, Thermo Fisher Scientific, USA) were applied and nuclei were stained with DAPI.

2.6. Terminal deoxynucleotidyl transferase dUTP nick end labeling (TUNEL) assay

We performed the TUNEL assay with an *in-situ* cell death detection kit (Roche, Germany) according to the manufacturer's instructions. Briefly, after rewarming at room temperature, slides were fixed with 4% paraformaldehyde for 30 min and subsequently soaked in 0.1% Triton X-100 for 5 min, followed by incubation with TUNEL reaction mixture for 60 min at 37 °C.

2.7. Cell culture of murine microglial cells BV2 and hippocampal neuronal cells HT22

Murine BV2 microglial cells were obtained from the Cell Resource Center of Peking Union Medical College (China) and cultured in Dulbecco's Modified Eagle's Medium (DMEM) supplemented with 10% fetal bovine serum (FBS). Murine hippocampal neuronal cells HT22 were purchased from the Bena Culture Collection (China) and cultured in DMEM/Nutrient Mixture F-12 supplemented with 10% FBS. All cells were incubated in a humidified atmosphere composed of 5% CO_2 at 37 °C.

2.8. Synthetic RNA oligonucleotide and siRNA transfection

MiR-23b mimics and inhibitors, miRNA negative control (miR-NC), scramble siRNA (si-control), ATG12 siRNA (si-ATG12), and Inositol Polyphosphate Multikinase siRNA (si-IPMK) were purchased from Genepharma (China). We transfected BV2 cells with Lipofectamine 3000 (Invitrogen, USA) according to the manufacturer's instructions. The sequences are listed in Supplementary Table 1.

2.9. mRFP-GFP-LC3 adenoviral infection

To track the autophagic flux, we infected BV2 cells with mRFP-GFP-LC3 adenovirus (HanBio, China). The BV2 cells were seeded on glass coverslips in 24-well plates and incubated overnight, and then infected with mRFP-GFP-LC3 adenovirus using polybrene. Cells were investigated under a fluorescence microscope (Olympus, Japan) after 48 h incubation and the numbers of autophagosomes (yellow puncta) and autolysosomes (red puncta) per cell were counted.

2.10. RNA extraction and reverse transcription quantitative PCR (RT-qPCR)

TRIzol™ reagent (Invitrogen, USA) was used to extract total RNA from the tissue and cells according to the manufacturer's instructions. Complementary DNA (cDNA) synthesis and subsequent RT-qPCR were performed using a reverse transcriptase kit [Takara Bio (Dalian) Co. Ltd., China] and a SYBR Green PCR kit [Takara Bio (Dalian) Co. Ltd., China], respectively. The primer sequences are provided in Supplementary Table 2.

2.11. Western blotting

Proteins from perihematomal tissue or cells were extracted and quantified with a bicinchoninic acid (BCA) protein assay kit (Beyotime Biotechnology, China). Equal quantities (in μg) of protein samples were separated by SDS-PAGE and transferred onto polyvinylidene fluoride (PVDF) membranes. The membranes were blocked with 5% non-fat milk for 1.5 h and probed with primary antibodies, including inducible isoform of nitric oxide synthase (iNOS;1:500; Santa Cruz Biotechnology), C—C Motif Chemokine Ligand 2(CCL2;1:1000;ProteintechGroup),Cleaved Caspase-3 (1:1000;ProteintechGroup), B-cell lymphoma 2(Bcl-2;1:1000;ProteintechGroup), ATG12 (1:1000;ProteintechGroup), sequestosome-1/P62(SQSTM1/P62;1:1000;ProteintechGroup), microtubule-associated protein 1 light chain 3 beta (LC3B; 1:1000;Cell Signaling Technology), Akt(1:1000; Cell Signaling Technology), phospho-Akt(p-Akt; 1:1000; Cell Signaling Technology), mammalian target of rapamycin (mTOR; 1:1000; Cell Signaling Technology), phospho-mTOR(p-mTOR; 1:1000; Cell Signaling Technology), and IPMK(1:1000; Abcam). β-actin (1:1000; Abcam) was used as an internal control. The secondary antibodies were goat anti-mouse or anti-rabbit IgG (H + L) HRP (1:5000; ProteintechGroup).

2.12. ELISA assay and nitric oxide (NO) assay

The levels of IL-6, IL-1β and TNF-α in cell culture supernatant were detected by ELISA (R&D Systems, USA) according to the manufacturer's instructions. The concentration of supernatant NO was quantified using a Nitric Oxide Assay Kit utilizing Griess Reagent (Beyotime Biotechnology) following the manufacturer's instructions.

2.13. Cell counting kit-8 assay

A cell counting kit-8 assay (CCK-8; Dojindo Molecular Technologies, Japan) was utilized to measure cell viability. Briefly, 10 μl of CCK-8 reagent was added to each well and the plate was incubated at 37 °C for 2 h. Cell viability was assessed by measuring absorbance at 450 nm using a microplate reader.

2.14. Flow cytometric analysis

Cell apoptosis was assessed using an Annexin V-PE/7ADD apoptosis detection kit (BD Biosciences, USA) by flow cytometry. In brief, after different treatments, cells were suspended in 1 × binding buffer and incubated with Annexin V-PE/7-ADD for 15 min at 25 °C in the dark. Then cell apoptosis was analyzed within 1 h using a flow cytometer (BD Biosciences).

2.15. Dual luciferase assay

TargetScan(http://www.targetscan.org/vert_72/), miRWalk (http://zmf.umm.uni-heidelberg.de/apps/zmf/mirwalk2/), miRDB (http://mirdb.org/), miRanda (http://www.microrna.org/microrna/home.do) were used to predict the target genes of miR-23b. Wild-type and mutant IPMK promoter luciferase plasmids containing sequences of the miR-23b target region (IPMK 3′UTR-WT/IPMK 3′UTR-MUT) were obtained from GeneChem. The sequences of IPMK 3′UTR-WT and IPMK 3′UTR-MUT are listed in Supplementary Table 3.We co-transfected 293 T cells with 0.1 μg IPMK 3′UTR-WT or IPMK 3′UTR-MUT and 0.4 μg miR-23b mimics or miR-NC respectively, using Lipofectamine 3000 (Invitrogen) in 24-well plates. Then, 48 h after transfection, luciferase activity was measured using the Dual-Luciferase reporter assay system (Promega, USA), as quantified by the ratio of Firefly/Renilla activity.

2.16. Statistical analysis

All experiments were conducted at least three times. All experimental data were expressed as mean ± standard deviation and were considered statistically significant when $p < 0.05$. Statistical significance between two groups was analyzed using two-tailed Student's *t*-test. Behavioral data were analyzed by Kruskal–Wallis test with Dunn's test for multiple comparisons. Continuous variables were analyzed by analysis of variance (ANOVA) with *post hoc* Newman-Keuls test. All data were analyzed using SPSS 22.0 (IBM Corp., USA) and GraphPad Prism 7.0 (GraphPad Software, USA). To determine the adequate sample size for each group, we performed a power analysis with G*Power 3.1.9.2 software at a 5% significance level and obtained a power level > 0.9.

3. Results

3.1. MiR-23b expression was significantly decreased in ICH in vivo and in vitro

To confirm miRNA array data from our previous study [27], we investigated the miR-23b expression of perihematomal tissue in ICH rats and sham ones on days 1, 3 and 5.Consistently, the results showed that on days 1, 3 and 5 after ICH, the levels of miR-23b in the ICH group were significantly lower than those in the sham group (Fig. 1A). Hemin, a cytotoxic decomposition product of hemoglobin following ICH, was used to mimic secondary injury of ICH *in vitro* [17]. We found miR-23b levels were significantly reduced in the hemin group compared with those in the control group (Fig. 1B), suggesting that miR-23b may be implicated in the pathogenesis of ICH.

3.2. Overexpression of miR-23b alleviated neurological function deficits and brain injury in ICH rats

To explore the regulatory role of miR-23b on ICH *in vivo*, LV-miR-23b was administered intracerebroventricularly to rats, and expression of miR-23b was quantified by RT-qPCR (Fig. 2A). Behavioral assessments were performed on days 1, 3 and 5 after ICH induction. We consistently found that the ICH group showed significantly increased frequencies of right turns and reduced limb placement scores compared with the sham group while LV-miR-23b administration improved the impaired neurological functions (Fig. 2B and C). To explore the effects of miR-23b on brain injury induced by ICH, we investigated the brain water content on day 3 after ICH and found that ICH induction significantly increased brain water content, which was further decreased by LV-miR-23b administration (Fig. 2D). Furthermore, histological examination showed a shrinking area of hematoma in the LV-miR-23b group compared with the LV-miR-NC group (Fig. 2E).

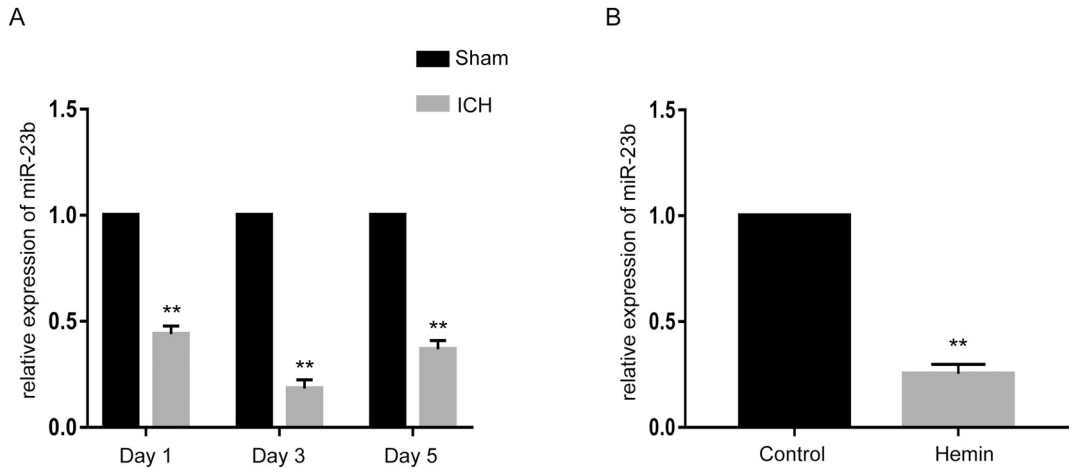

Fig. 1. MiR-23b expression was significantly decreased in ICH models *in vivo* and *in vitro*. (A) MiR-23b expression of perihematoma area on days 1, 3 and 5 after ICH detected by RT-qPCR. (B) MiR-23b expression in BV2 cells under hemin-stimulation. $^{**}p < 0.01$.Datas are representative of at least three independent experiments.

3.3. Overexpression of miR-23b attenuated microglia activation, neuroinflammation and neuronal apoptosis in ICH rats

We performed Iba1-staining using immunofluorescence for detecting microglia activation and noticed that the numbers of Iba1-positive microglia were markedly increased in the ICH group but was significantly reduced by LV-miR-23b administration (Fig. 3A). Additionally, LV-miR-23b led to a significant decrease in expression of the inflammation factors iNOS and CCL2 compared with LV-miR-NC group (Fig. 3B). Immunofluorescence staining of NeuN showed that ICH induction decreased the number of neurons in the perihematomal area, while LV-miR-23b administration led to an increase (Fig. 3C). The TUNEL assay showed increased apoptosis in the ICH group, which decreased by LV-miR-23b administration (Fig. 3D). Western blotting of Cleaved Caspase-3 and Bcl-2 further confirmed that overexpression of miR-23b reduced apoptosis in ICH rats (Fig. 3B).

3.4. Overexpression of miR-23b suppressed inflammation in hemin-stimulated BV2 cells

To investigate the role of miR-23b in the inflammatory response stimulated by hemin, we transfected BV2 cells with miR-23b mimics, inhibitors, or negative control under hemin treatment and evaluated the expression of miR-23b by RT-qPCR (Fig. 4A). Next, we investigated the expression of the inflammation markers IL-6, IL-1β, TNF-α, iNOS and CCL2, we found that hemin stimulation could markedly increase these inflammation markers. Additionally, overexpression of miR-23b in BV2 cells led to a reduction in IL-6, IL-1β, TNF-α and NO expression in the supernatant, as measured by ELISA and Griess reagent, and a decrease of iNOS and CCL2 expression, as measured using western blotting. However, inhibition of miR-23b resulted in opposite effects (Fig. 4B and C). Together, our results reveal that overexpression of miR-23b ameliorates inflammation stimulated by hemin in BV2 cells.

3.5. Overexpression of miR-23b prevented neuronal apoptosis induced by hemin-stimulated BV2 cells

To investigate the effects of BV2 microglial cells on HT22 neuronal cells after hemin stimulation, we established neuronal and microglial co-cultures. We observed a significant decrease in HT22 cell viability after treatment with hemin-stimulated BV2 cell supernatant. However, the CCK8 assay demonstrated that the supernatant of hemin-induced BV2 cells transfected with miR-23b mimics showed less cytotoxicity to HT22 cells (Fig. 4D). Testing for apoptosis showed similar results, and the apoptosis rate of HT22 cells was significantly increased by the hemin-stimulated BV2 cell supernatant; however, transfection with miR-23b mimics in BV2 cell culture was able to mitigate co-cultured HT22 cell apoptosis, and inhibition of miR-23b led to aggravation in apoptosis (Fig. 4E).

3.6. MiR-23b directly targeted IPMK and suppressed autophagy activity

The target genes of miR-23b were identified using *in silico* target prediction tools, including TargetScan, miRWalk, miRDB and miRanda (Fig. 5A). Among those target genes, IPMK was selected for the subsequent experiments (Fig. 5B). Indeed, we found that IPMK contains a highly conserved putative miR-23b binding site in its 3′UTR region (Fig. 5C) and the luciferase reporter assay with the 3′UTR of IPMK containing putative or mutated miR-23b recognition elements further confirmed that IPMK was a direct target of miR-23b (Fig. 5D). Furthermore, western blotting showed that overexpression of miR-23b significantly reduced IPMK expression, while inhibition of miR-23b increased IPMK expression (Fig. 5E), indicating miR-23b negatively regulates IPMK protein expression.

Given IPMK is necessary for autophagy [31], we further explored whether autophagy activity was regulated by miR-23b in hemin-stimulated cells. We found that overexpression of miR-23b led to a significant decrease in LC3-II protein levels and an accumulation of P62, whereas inhibition of miR-23b yielded opposite results (Fig. 5E). Consistently, overexpression of miR-23b decreased the numbers of mRFP-LC3-labeled puncta (representing autolysosomes) and yellow puncta (representing autophagosomes), but inhibition of miR-23b increased both red and yellow puncta (Fig. 5F). These results suggest that overexpression of miR-23b suppressed autophagy flux, which may be associated with negative regulation of IPMK.

3.7. Silencing of IPMK alleviated the effects of miR-23b inhibitors

To further evaluate whether IPMK mediates the effects of miR-23b in hemin-stimulated cells, we conducted a series of rescue experiments in BV2 cells. First, we evaluated the silencing efficiency of si-IPMK by RT-qPCR and western blotting (Fig. 6A, left and Fig. 6B, upper). Second, we observed that silencing of IPMK attenuated the increase in supernatant inflammatory markers of IL-6, IL-1β, TNF-α and NO, as well as the expression of iNOS and CCL2 in BV2 cells transfected with miR-23b inhibitors (Fig. 6C and D). Additionally, we found that the silencing of IPMK abrogated the effects of miR-23b inhibitors on the expression of autophagy-related genes LC3B and P62 (Fig. 6D). Furthermore, co-transfection of si-IPMK and miR-23b inhibitors in BV2 cells mitigated co-cultured HT22 cell apoptosis (Fig. 6E). These results collectively

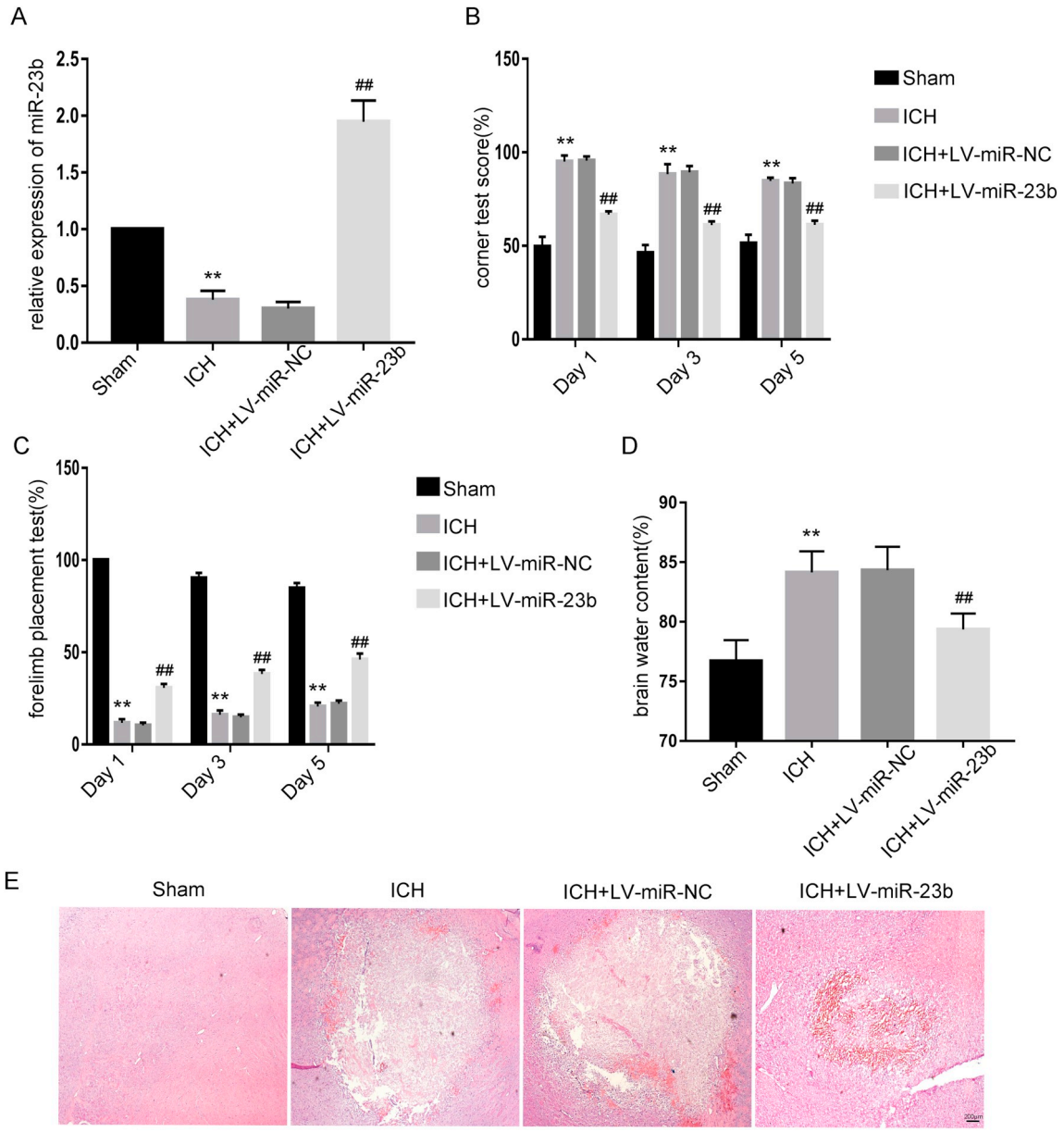

Fig. 2. Overexpression of miR-23b improved neurological function and alleviated brain injury in ICH rats. (A) MiR-23b expression was detected by RT-qPCR. (B) Corner tests were performed on days 1, 3 and 5(n = 6). (C) Forelimb placement tests were performed on days 1, 3 and 5 (n = 6). (D) Brain water content was measured on day 3 after ICH (n = 6). (E) Hematoxylin and eosin staining of hematoma area on day 3 after ICH. $^{**}p < 0.01$ *versus* the sham group; $^{\#\#}p < 0.01$ *versus* the ICH + LV-miR-NC group.

show that IPMK mediates the effects of miR-23b on inflammation and autophagy of BV2 cells while influencing the survival of co-cultured HT22 cells.

3.8. The Akt/mTOR/autophagy pathway mediated the effects of miR-23b

To further explore whether autophagy plays a role in the inflammation regulation by miR-23b in hemin-stimulated cells, we used both the autophagy inhibitor chloroquine (CQ) and the siRNA against ATG12 (Fig. 6A, right and Fig. 6B, lower). First, we observed that miR-23b inhibitors in the presence of CQ further increased LC3-II levels compared with CQ alone, further confirming that miR-23b negatively regulates autophagy flux. Second, the effects of miR-23b inhibitors on LC3-II and P62 levels were attenuated by si-ATG12, indicating that miR-23b suppresses autophagy, which might mechanically be associated with the regulation of ATG12. Third, we found that si-ATG12 and CQ both successfully reversed the effects of miR-23b inhibitors on inflammation and showed effects similar to si-IPMK (Fig. 6C and D). These results suggest that excessive inflammation could be alleviated by inhibition of autophagy, further implying that the attenuation of neuroinflammation by miR-23b is modulated at least partly by directly targeting IPMK and inhibiting autophagy.

As the Akt/mTOR pathway is a classical autophagy signaling pathway, we next investigated several critical proteins expression in the different groups. We found that miR-23b mimics significantly increased the expression of p-Akt and p-mTOR, and downregulated the expression of IPMK in BV2 cells cultured under hemin stimulation, while miR-23b inhibitors yielded contrary results (Fig. 6F).

4. Discussion

Intracerebral hemorrhage is a devastating cerebral disease with high

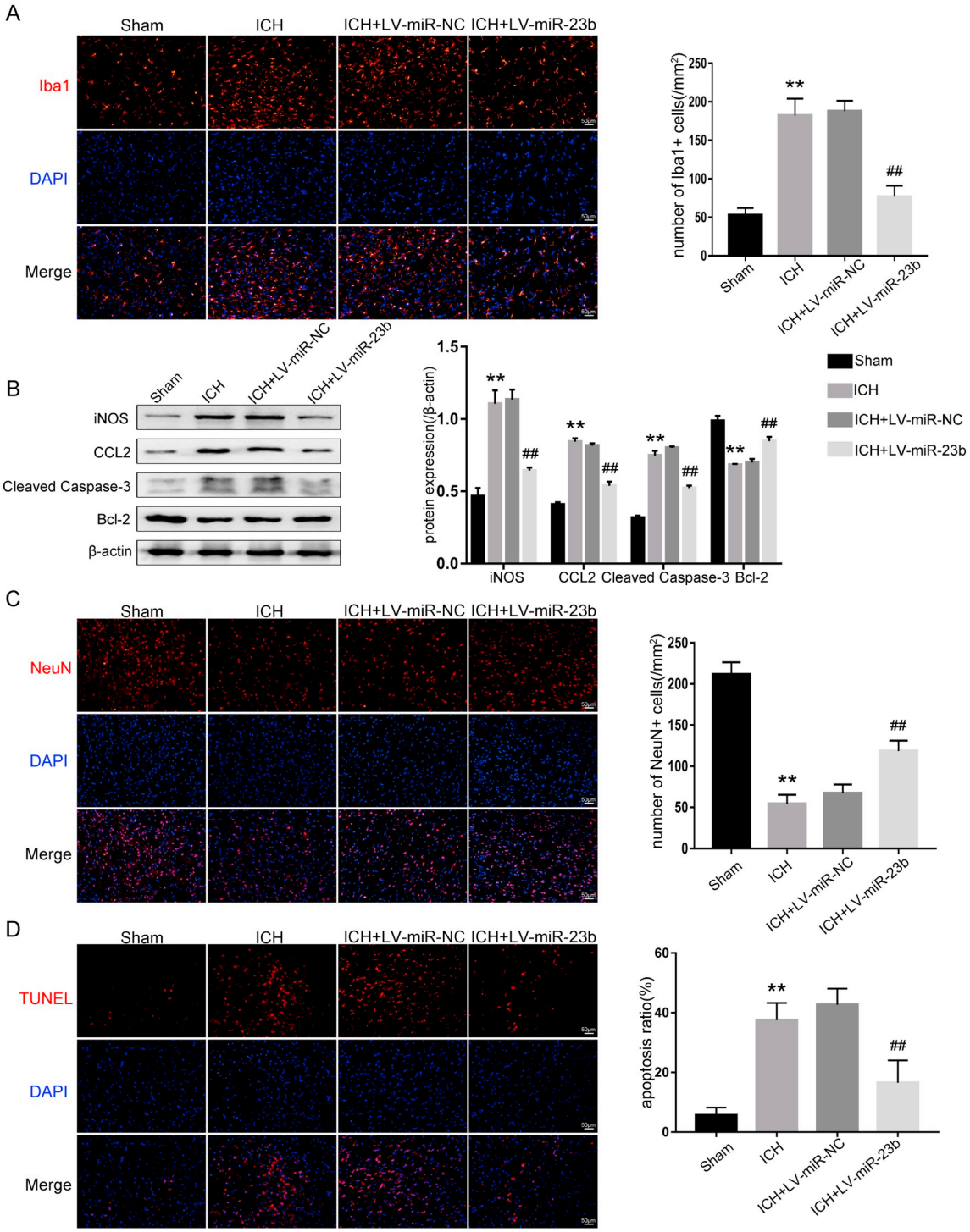

Fig. 3. Overexpression of miR-23b attenuated microglia activation, neuroinflammation and neurons apoptosis in ICH rats. (A) Microgila activation was detected by immunofluorescence staining of Iba1. (B) Western blotting analysis of the expression levels of iNOS, CCL2, Cleaved caspase-3 and Bcl-2. (C) Immunofluorescence staining of neurons marker NeuN. (D) Apoptotic cells were detected using TUNEL assay. $^{**}p < 0.01$ *versus* the sham group; $^{\#\#}p < 0.01$ *versus* the ICH + LV-miR-NC group.

morbidity and mortality [1]. Increasing evidence suggests that neuroinflammation plays a critical role in the progression and prognosis of ICH [32,33], which induces oxidative stress, increases production of ROS, increases the permeability of the blood-brain barrier and brain edema, ultimately leads to brain injuries and neurological deterioration [7,14]. Therefore, neuroinflammation is considered to be an important target for ICH therapy. Accumulating evidence suggests that miRNAs play critical roles in ICH therapy [34,35]. In the present study, we observed miR-23b was significantly decreased in ICH models *in vivo* and *in vitro*, which is in accordance with the previous miRNA chip array of serum from patients with ICH [27]. Importantly, we first explored the potential neuroprotective role of miR-23b in ICH and found that exogenous miR-23b overexpression alleviated neurological function deficits, as revealed by corner tests and forelimb placement tests, and attenuated brain injuries including brain water content and hematoma area in ICH rats. Although previous studies have demonstrated that

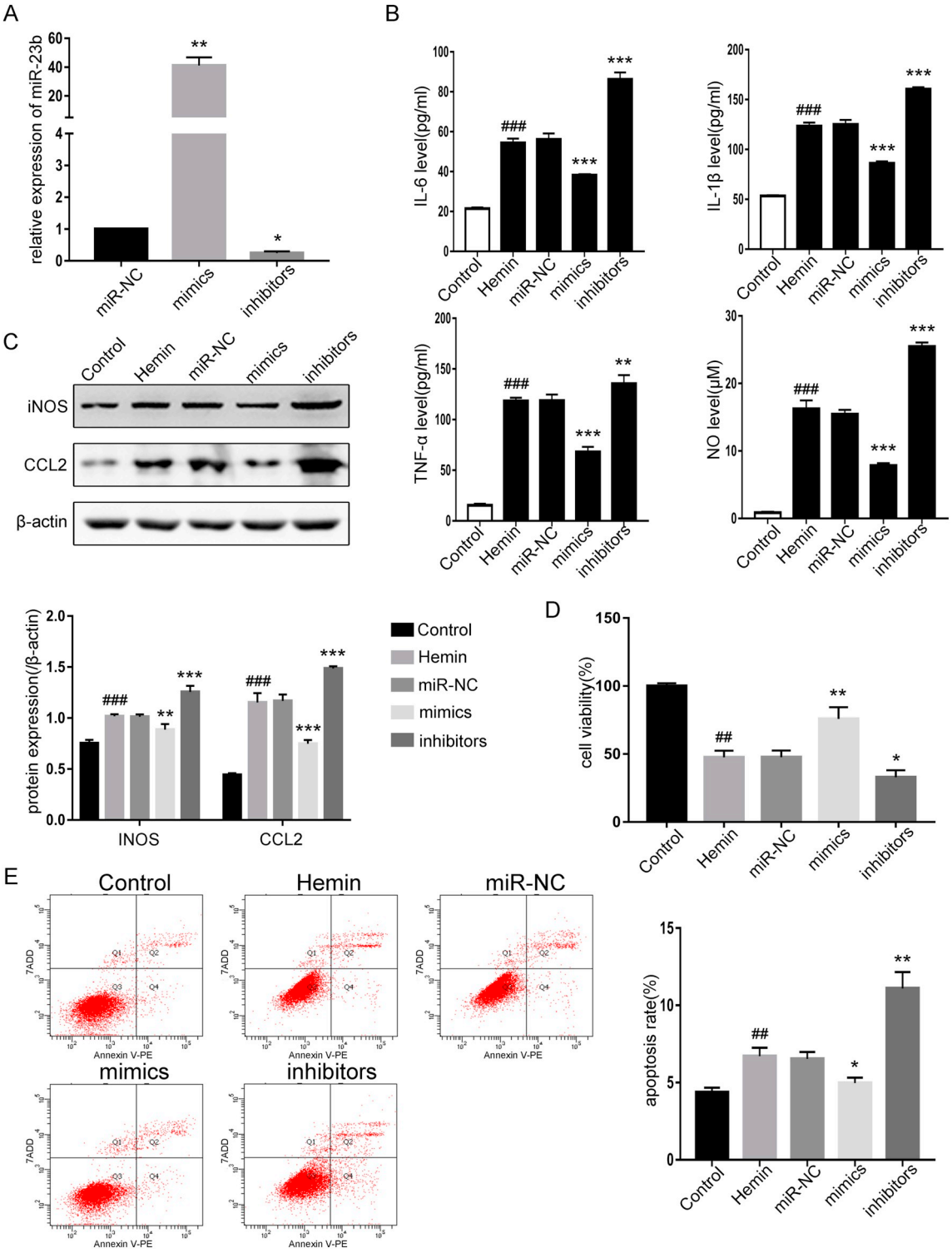

Fig. 4. Overexpression of miR-23b suppressed hemin-stimulated inflammation in microglial cells BV2 and prevented co-cultured neuronal cells HT22 apoptosis. (A) MiR-23b expression detected by qPCR after transfection under hemin stimulation. (B) Expression levels of IL-6, IL-1β, TNF-α and NO in BV2 supernatant using ELISA assay and Griess reagent. (C) Western blotting of iNOS and CCL2 in BV2 cells of control group, hemin group and transfection group within hemin stimulation. (D) Viability of HT22 co-cultured with BV2 in different groups using CCK8 assay. (E) HT22 apoptosis analyzed by Annexin V-PE/7ADD detection kit in different groups. $^{\#\#}p < 0.01$, $^{\#\#\#}p < 0.001$ *versus* the control group;$^{*}p < 0.05$, $^{**}p < 0.01$, $^{***}p < 0.001$ *versus* the miR-NC transfection group under hemin stimulation.

miR-23b exerted an anti-inflammatory role in IL-17 associated autoimmune inflammation [36], experimental autoimmune encephalomyelitis [26], and sepsis-induced cardiomyopathy [37], it is unclear whether miR-23b can regulate neuroinflammation to protect against ICH. Interestingly, we found that overexpression of miR-23b could suppress the activation of microglia and decrease expression of inflammation factors, thus mitigating ICH-induced neuroinflammation *in vivo*. Hemin, a hematoma degradation product, rapidly released following ICH, is known to powerfully activate microglia *via* TLR4 [38] and to mimic ICH conditions *in vitro* [17]. We observed that

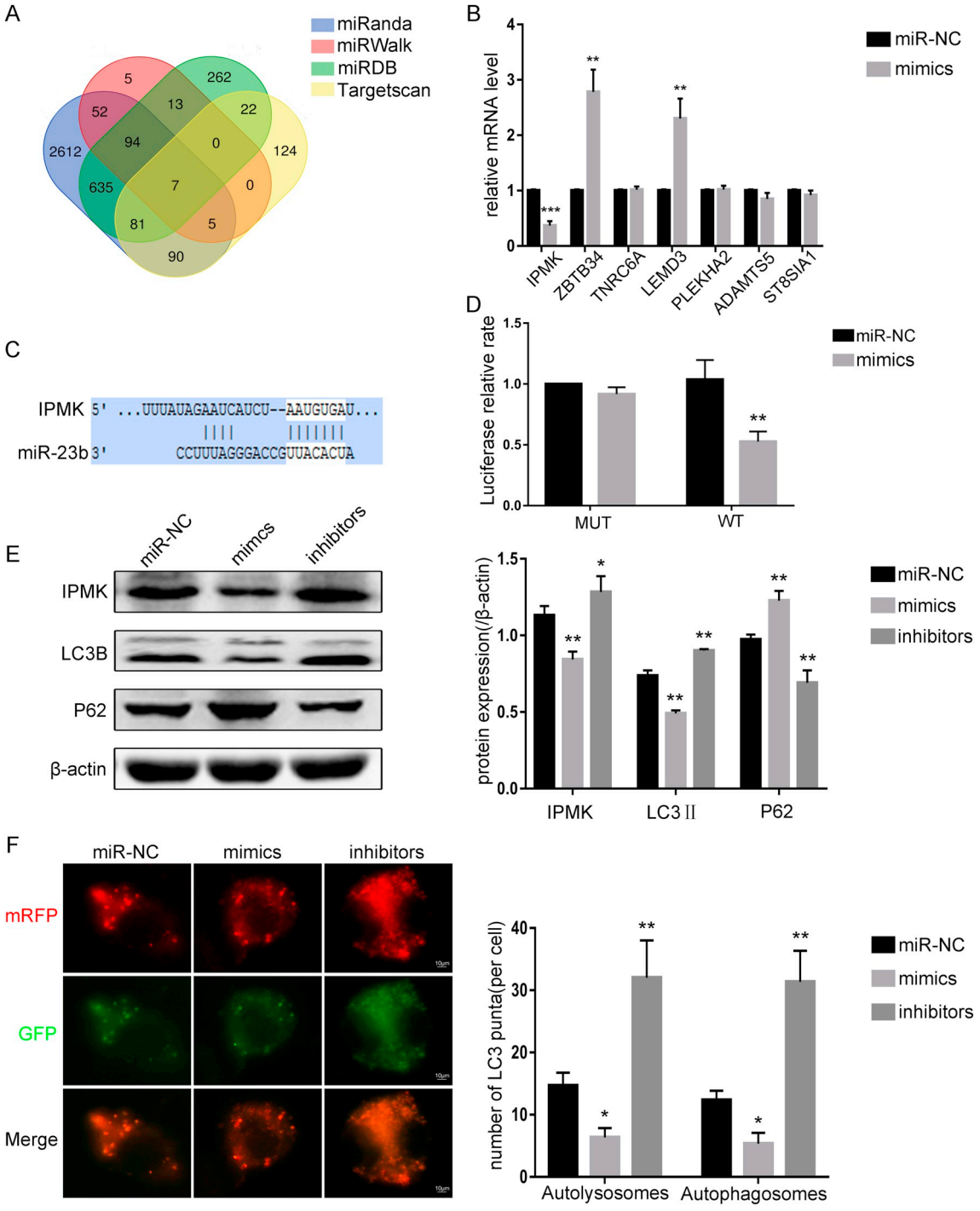

Fig. 5. MiR-23b directly targeted IPMK and negatively regulated autophagy activity. (A) Predicted target genes of miR-23b integrated by four *in silico* prediction tools. (B) Relative mRNA levels of the predicted target genes detected by qPCR after transfection of miR-23b mimics in BV2. (C) Target region between miR-23b and IPMK. (D) Luciferase report assay for binding of miR-23b and IPMK. (E) Western blotting of IPMK, LC3B and P62 in BV2 after transfection with miR-23b mimics, inhibitors or miR-NC. (F) Immunofluorescence images of LC3 puncta in BV2 cells transfected with miR-23b mimics, inhibitors or miR-NC. Red puncta represent autolysosomes, yellow puncta represent autophagosomes.*$p < 0.05$, **$p < 0.01$, ***$p < 0.001$ *versus* the miR-NC group. (For interpretation of the references to colour in this figure legend, the reader is referred to the web version of this article.)

overexpression of miR-23b decreased hemin-stimulated inflammatory markers levels in cultured BV2 microglial cells, further implying miR-23b exerts anti-inflammation effects and plays a protective role against ICH.

Besides the anti-inflammation effects of miR-23b, overexpression of miR-23b could reduce neuronal death, as revealed by an increase in the number of NeuN-(neuronal cell marker) positive cells. A recent study of collagenase-induced ICH has demonstrated that neurons are highly vulnerable to damage, while most microglia and astrocytes are relatively resistant in the first 24 to 72 h after ICH [39]. Therefore, the decreased number of TUNEL-positive cells in LV-miR-23b group may indicate the mitigation of neuronal apoptosis by miR-23b administration, further suggesting that miR-23b may exert a pro-survival effect on neurons, both directly, by attenuating neuronal apoptosis, and indirectly, by influencing the surrounding cells, including microglial cells, which in turn promote neuronal survival. Previous research suggests

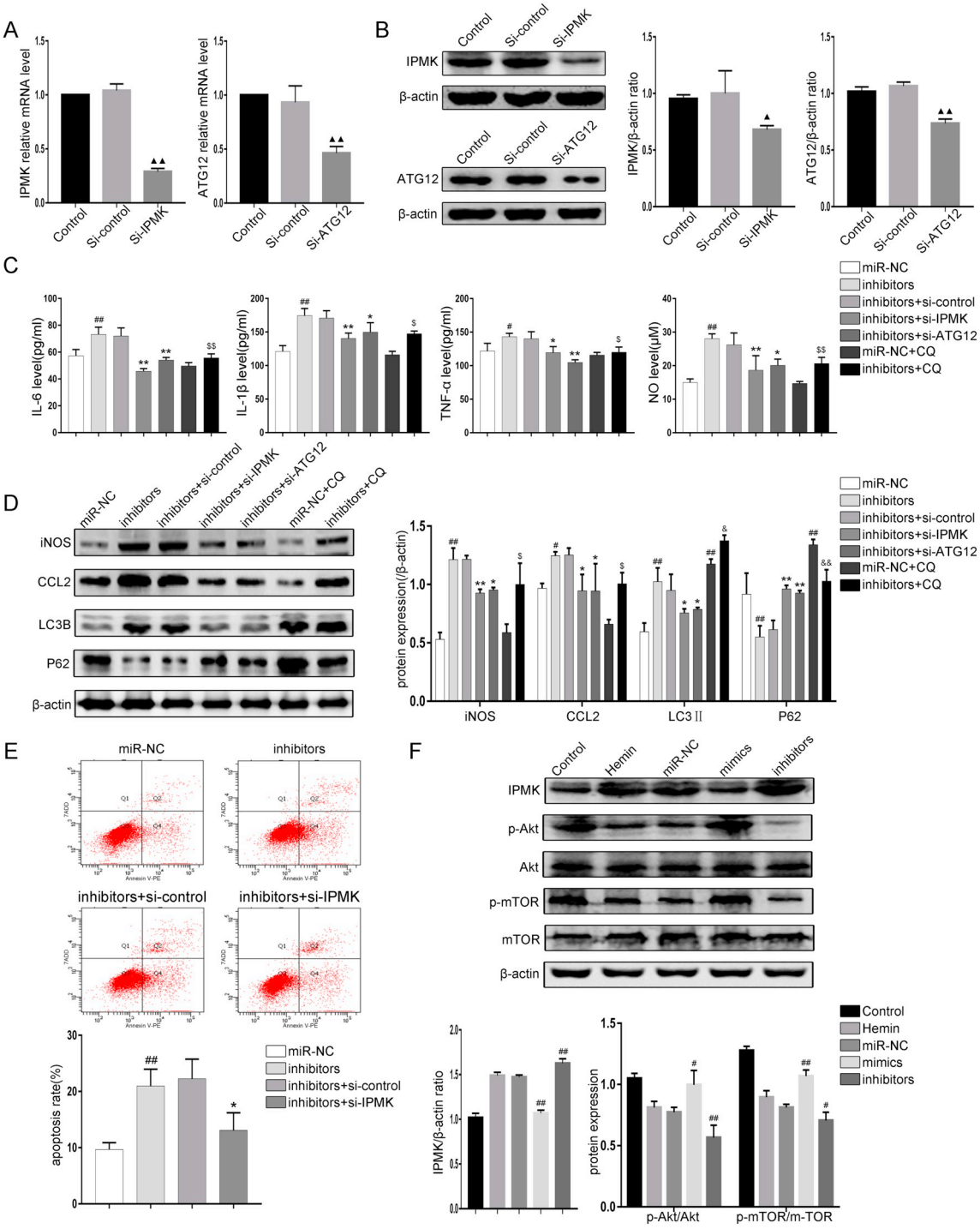

Fig. 6. Silence of IPMK alleviated the effects of miR-23b inhibitors and the Akt/mTOR autophagy pathway was involved in the regulation of miR-23b. (A) Relative mRNA levels of IPMK and ATG12 in BV2 after transfection with si-IPMK or si-ATG12. (B) Western blotting of IPMK and ATG12 in BV2 after transfection with si-IPMK or si-ATG12. (C) Expression levels of IL-6, IL-1β, TNF-α and NO in BV2 supernatant using ELISA assay and Griess reagent. (D) Western blotting of iNOS, CCL2,LC3B and P62 in BV2 after transfection with miR-NC, miR-23b inhibitors alone, miR-23b inhibitors with si-control, miR-23b inhibitors with si-IPMK, miR-23b inhibitors with si-ATG12, miR-NC together with chloroquine (CQ) incubation, or miR-23b inhibitors together with CQ incubation. (E) Apoptosis of HT22 co-cultured with BV2 was detected by Annexin V-PE/7ADD detection kit in different groups. (F) Western blotting of IPMK, p-Akt, Akt, p-mTOR and mTOR in BV2 of different groups. $^{▲}p < 0.05$, $^{▲▲}p < 0.01$ *versus* the si-control transfection group; $^{\#}p < 0.05$, $^{\#\#}p < 0.01$ *versus* the miR-NC group; $^{\$}p < 0.05$, $^{\$\$}p < 0.01$ *versus* the miR-23b inhibitors group; $^{*}p < 0.05$, $^{**}p < 0.01$ *versus* the miR-23b inhibitors + si-control transfection group; $^{\&}p < 0.05$, $^{\&\&}p < 0.01$ *versus* the miR-NC + chloroquine (CQ) group.

that inflammation response induced by ICH can promote BBB breakdown and continuous glutamate infiltration, which results in excessive neuronal calcium load and initiates neuronal cell death [40]. In our study, we observed that overexpression of miR-23b in hemin-stimulated microglial BV2 cells can attenuate co-cultured neuronal cells HT22 death, further confirming the indirect anti-apoptotic effect of miR-23b on neurons.

MiRNAs are known to modulate diverse biological and pathological

processes by direct interaction with the 3′UTR region of the target genes [20]. Hence, to further explore the specific molecular mechanisms of miR-23b in ICH, we performed a gain- and loss-of-function analysis and luciferase reporter assay. We demonstrated that overexpressed miR-23b inhibited the expression of IPMK, by reducing the stability of the mRNA and suppressing protein translation, and we confirmed IPMK as a direct target of miR-23b.IPMK, a member of the IPK-superfamily kinases, plays critical catalytic-dependent roles in catalyzing phosphorylation of inositols and functions physiologically as a phosphoinositide 3-kinase, which forms phosphatidylinositol 3,4,5-trisphosphate (PIP3) [41]. IPMK also has important non-catalytic functions in diverse diseases, partly through interactions with TRAF6 [42], p53 [43], and AMPK [44]. Notably, several studies have explored the role of IPMK in regulating autophagy in liver diseases and have emphasized that IPMK plays a determinate role in autophagy [31,45]. In the current study, our results of western blotting of autophagic-related genes (LC3B, P62) and immunofluorescence images of LC3 showed overexpression of miR-23b suppressed autophagy flux induced by hemin, and we observed that the autophagy modulation of miR-23b might mechanically be associated with ATG12,an essential protein for the formation of autophagosomes. Moreover, to evaluate the IPMK role on the effects of miR-23b, we performed a series of rescue experiments using si-IPMK, and the results demonstrated that IPMK participated in cell inflammation, autophagy and apoptosis, further indicating that miR-23b exerted anti-inflammation and autophagy-inhibition effects on BV2 cells and promoted the survival of co-cultured HT22 cells through suppression of IPMK.

Autophagy has been increasingly shown to play a critical role in controlling inflammation and apoptotic signaling in ICH. Indeed, suppression of autophagy has been reported to decrease microglial activation and inflammation in ICH [46]. For example, 3-Methyladenine (3-MA), an inhibitor of the autophagy pathway, can suppress apoptosis and neuroinflammation to exert neuroprotective effects after ICH [18,19]. Mechanistically, autophagy could control IL-1β secretion by targeting pro-IL-1β for lysosomal degradation and regulate activation of the NLRP3 inflammasome [47]. To further determine whether autophagy was involved in regulation of inflammation by miR-23b, we used the autophagy inhibitor chloroquine(CQ) and siRNA against ATG12 in our ICH models *in vitro*. Our results demonstrated that si-ATG12 and CQ both could reverse the effects of miR-23b inhibitors on inflammation in hemin-stimulated BV2 cells, yielding an effect similar to the influence of si-IPMK. These results indicate that excessive inflammation could be alleviated by inhibition of autophagy, further implying that neuroinflammation alleviation by miR-23b is at least partially mediated by targeting IPMK and inhibiting autophagy.

The Akt/mTOR signaling pathway, an indispensable cascade, has been implicated in cell growth, apoptosis and migration [48–50]. Furthermore, this pathway has been reported to exert a critical role in autophagy regulation, and activation of Akt/mTOR pathway can negatively regulate autophagy [51]. In the present study, we observed that miR-23b mimics increased Akt and mTOR phosphorylation and downregulated IPMK in hemin-stimulated BV2 cells, whereas miR-23b inhibitors showed opposite effects. These results suggest that miR-23b negatively regulates IPMK-mediated autophagy *via* activation of the Akt/mTOR signaling pathway. Some researchers have demonstrated that activation of the AKT/mTOR pathway improved myelination growth by upregulating PTEN [52] and attenuated neuronal apoptosis by modulating intracellular-free calcium level [53], indicating that activation of the AKT/mTOR pathway plays a protective role in neurological disease. Overall, these findings further suggest that miR-23b might exert its anti-inflammation role in ICH through activating the Akt/mTOR signaling pathway by first targeting IPMK. However, as our study does not fully elucidate the specific mechanisms between IPMK and the Akt/mTOR pathway, we plan to explore this area in future studies.

Our results must be considered alongside the study limitations. Although we utilized the most commonly used model that most resembles the clinical ICH [7], the collagenase VII treatment *in vivo* may have induced exaggerated inflammation. Additionally, BV2 microglial cells and HT22 hippocampal neuronal cells are derived cell lines that are typically used *in vitro* for ICH experiments [32,54], but still cannot replace experiments involving primary cells. Furthermore, in the current study, we investigated IPMK as a novel target gene of miR-23b that could mediate the role of miR-23b in ICH neuroinflammation through the Akt/mTOR/autophagy pathway. However, there may be other mechanisms through which IPMK influences miR-23b neuroprotection that remain unclear and should, therefore, be explored in future studies.

In conclusion, our study demonstrated that overexpression of miR-23b alleviated neurological function deficits, brain injury and neuroinflammation in a rat ICH model, and attenuated inflammation of BV2 cells and apoptosis of co-cultured HT22 cells under hemin stimulation *in vitro*. In addition, we first confirmed IPMK was a functional target of miR-23b and mediated the role of miR-23b in ICH neuroinflammation at least partially through the Akt/mTOR /autophagy pathway. Ultimately, these findings imply that miR-23b-overexpression may provide a novel therapeutic intervention for patients suffering from ICH.

Author contributions

Liuting Hu performed the experiments and wrote the original paper; all authors analyzed the data; Zhiyi He designed the study and examined the paper. All authors agree to be accountable for the work content.

Funding

This work was supported by the National Natural Science Foundation of China [grant number 81571120].

Declaration of competing interest

The authors report no conflicts of interest.

Appendix A. Supplementary data

Supplementary data to this article can be found online at https://doi.org/10.1016/j.intimp.2019.105887.

References

[1] A.I. Qureshi, A.D. Mendelow, D.F. Hanley, Intracerebral haemorrhage, Lancet 373 (2009) 1632–1644.
[2] X. Hu, C. Tao, Q. Gan, J. Zheng, H. Li, C. You, Oxidative stress in intracerebral hemorrhage: sources, mechanisms, and therapeutic targets, Oxidative Med. Cell. Longev. 2016 (2016) 3215391.
[3] J.S. Kim-Han, S.J. Kopp, L.L. Dugan, M.N. Diringer, Perihematomal mitochondrial dysfunction after intracerebral hemorrhage, Stroke 37 (2006) 2457–2462.
[4] H. Zhao, Y. Chen, H. Feng, P2X7 receptor-associated programmed cell death in the pathophysiology of hemorrhagic stroke, Curr. Neuropharmacol. 16 (2018) 1282–1295.
[5] E. Mracsko, R. Veltkamp, Neuroinflammation after intracerebral hemorrhage, Front. Cell. Neurosci. 8 (2014) 388.
[6] Z. Zhang, Z. Zhang, H. Lu, Q. Yang, H. Wu, J. Wang, Microglial polarization and inflammatory mediators after intracerebral hemorrhage, Mol. Neurobiol. 54 (2017) 1874–1886.
[7] H. Zhu, Z. Wang, J. Yu, X. Yang, F. He, Z. Liu, et al., Role and mechanisms of cytokines in the secondary brain injury after intracerebral hemorrhage, Prog. Neurobiol. 178 (2019) 101610.
[8] J. Zhang, X. Shi, N. Hao, Z. Chen, L. Wei, L. Tan, et al., Simvastatin reduces neutrophils infiltration into brain parenchyma after intracerebral hemorrhage via regulating peripheral neutrophils apoptosis, Front. Neurosci. 12 (2018) 977.
[9] H. Zhao, T. Garton, R.F. Keep, Y. Hua, G. Xi, Microglia/macrophage polarization after experimental intracerebral hemorrhage, Transl. Stroke Res. 6 (2015) 407–409.
[10] X. Li, T. Wang, D. Zhang, H. Li, H. Shen, X. Ding, et al., Andrographolide ameliorates intracerebral hemorrhage induced secondary brain injury by inhibiting neuroinflammation induction, Neuropharmacology 141 (2018) 305–315.
[11] L. Zhao, S. Chen, P. Sherchan, Y. Ding, W. Zhao, Z. Guo, et al., Recombinant CTRP9 administration attenuates neuroinflammation via activating adiponectin receptor 1

after intracerebral hemorrhage in mice, J. Neuroinflammation 15 (2018) 215.
[12] Z.Q. Chen, H. Yu, H.Y. Li, H.T. Shen, X. Li, J.Y. Zhang, et al., Negative regulation of glial Tim-3 inhibits the secretion of inflammatory factors and modulates microglia to antiinflammatory phenotype after experimental intracerebral hemorrhage in rats, CNS neuroscience & therapeutics 25 (2019) 674–684.
[13] Y. Zhang, B. Yi, J. Ma, L. Zhang, H. Zhang, Y. Yang, et al., Quercetin promotes neuronal and behavioral recovery by suppressing inflammatory response and apoptosis in a rat model of intracerebral hemorrhage, Neurochem. Res. 40 (2015) 195–203.
[14] Y.Y. Hu, M. Huang, X.Q. Dong, Q.P. Xu, W.H. Yu, Z.Y. Zhang, Ginkgolide B reduces neuronal cell apoptosis in the hemorrhagic rat brain: possible involvement of Toll-like receptor 4/nuclear factor-kappa B pathway, J. Ethnopharmacol. 137 (2011) 1462–1468.
[15] S. Hu, G. Xi, H. Jin, Y. He, R.F. Keep, Y. Hua, Thrombin-induced autophagy: a potential role in intracerebral hemorrhage, Brain Res. 1424 (2011) 60–66.
[16] X.C. Duan, W. Wang, D.X. Feng, J. Yin, G. Zuo, D.D. Chen, et al., Roles of autophagy and endoplasmic reticulum stress in intracerebral hemorrhage-induced secondary brain injury in rats, CNS neuroscience & therapeutics 23 (2017) 554–566.
[17] X. Shen, L. Ma, W. Dong, Q. Wu, Y. Gao, C. Luo, et al., Autophagy regulates intracerebral hemorrhage induced neural damage via apoptosis and NF-kappaB pathway, Neurochem. Int. 96 (2016) 100–112.
[18] Z. Yang, B. Liu, L. Zhong, H. Shen, C. Lin, L. Lin, et al., Toll-like receptor-4-mediated autophagy contributes to microglial activation and inflammatory injury in mouse models of intracerebral haemorrhage, Neuropathol. Appl. Neurobiol. 41 (2015) e95–106.
[19] P. Chang, W. Dong, M. Zhang, Z. Wang, Y. Wang, T. Wang, et al., Anti-necroptosis chemical necrostatin-1 can also suppress apoptotic and autophagic pathway to exert neuroprotective effect in mice intracerebral hemorrhage model, Journal of molecular neuroscience : MN 52 (2014) 242–249.
[20] V. Ambros, The functions of animal microRNAs, Nature 431 (2004) 350–355.
[21] B. Yuan, H. Shen, L. Lin, T. Su, L. Zhong, Z. Yang, MicroRNA367 negatively regulates the inflammatory response of microglia by targeting IRAK4 in intracerebral hemorrhage, J. Neuroinflammation 12 (2015) 206.
[22] Y. Zhang, B. Han, Y. He, D. Li, X. Ma, Q. Liu, et al., MicroRNA-132 attenuates neurobehavioral and neuropathological changes associated with intracerebral hemorrhage in mice, Neurochem. Int. 107 (2017) 182–190.
[23] S. Naidu, L. Shi, P. Magee, J.D. Middleton, A. Lagana, S. Sahoo, et al., PDGFR-modulated miR-23b cluster and miR-125a-5p suppress lung tumorigenesis by targeting multiple components of KRAS and NF-kB pathways, Sci. Rep. 7 (2017) 15441.
[24] P. Qi, M.D. Xu, X.H. Shen, S.J. Ni, D. Huang, C. Tan, et al., Reciprocal repression between TUSC7 and miR-23b in gastric cancer, Int. J. Cancer 137 (2015) 1269–1278.
[25] S. Majid, A.A. Dar, S. Saini, S. Arora, V. Shahryari, M.S. Zaman, et al., miR-23b represses proto-oncogene Src kinase and functions as methylation-silenced tumor suppressor with diagnostic and prognostic significance in prostate cancer, Cancer Res. 72 (2012) 6435–6446.
[26] Y. Zhang, J.J. Han, X.Y. Liang, L. Zhao, F. Zhang, J. Rasouli, et al., miR-23b Suppresses Leukocyte Migration and Pathogenesis of Experimental Autoimmune Encephalomyelitis by Targeting CCL7. Molecular Therapy : The Journal of the American Society of Gene Therapy, vol. 26, (2018), pp. 582–592.
[27] Y. Zhu, J.L. Wang, Z.Y. He, F. Jin, L. Tang, Association of altered serum microRNAs with perihematomal edema after acute intracerebral hemorrhage, PLoS One 10 (2015) e0133783.
[28] F. Li, B. Yang, T. Li, X. Gong, F. Zhou, Z. Hu, HSPB8 over-expression prevents disruption of blood-brain barrier by promoting autophagic flux after cerebral ischemia/reperfusion injury, J. Neurochem. 148 (2019) 97–113.
[29] G.A. Rosenberg, S. Mun-Bryce, M. Wesley, M. Kornfeld, Collagenase-induced intracerebral hemorrhage in rats, Stroke 21 (1990) 801–807.
[30] T. Xi, F. Jin, Y. Zhu, J. Wang, L. Tang, Y. Wang, et al., miR-27a-3p protects against blood-brain barrier disruption and brain injury after intracerebral hemorrhage by targeting endothelial aquaporin-11, J. Biol. Chem. 293 (2018) 20041–20050.
[31] P. Guha, R. Tyagi, S. Chowdhury, L. Reilly, C. Fu, R. Xu, et al., IPMK mediates activation of ULK signaling and transcriptional regulation of autophagy linked to liver inflammation and regeneration, Cell Rep. 26 (2019) 2692–2703 (e7).
[32] C.H. Wu, S.K. Shyue, T.H. Hung, S. Wen, C.C. Lin, C.F. Chang, et al., Genetic deletion or pharmacological inhibition of soluble epoxide hydrolase reduces brain damage and attenuates neuroinflammation after intracerebral hemorrhage, J. Neuroinflammation 14 (2017) 230.
[33] X. Yang, J. Sun, T.J. Kim, Y.J. Kim, S.B. Ko, C.K. Kim, et al., Pretreatment with low-dose fimasartan ameliorates NLRP3 inflammasome-mediated neuroinflammation and brain injury after intracerebral hemorrhage, Exp. Neurol. 310 (2018) 22–32.
[34] D. Guo, J. Liu, W. Wang, F. Hao, X. Sun, X. Wu, et al., Alteration in abundance and compartmentalization of inflammation-related miRNAs in plasma after intracerebral hemorrhage, Stroke 44 (2013) 1739–1742.
[35] X. Cheng, B.P. Ander, G.C. Jickling, X. Zhan, H. Hull, F.R. Sharp, et al., MicroRNA and their target mRNAs change expression in whole blood of patients after intracerebral hemorrhage, Journal of cerebral blood flow and metabolism : official journal of the International Society of Cerebral Blood Flow and Metabolism (2019) 271678X19839501, , https://doi.org/10.1177/0271678X19839501.
[36] S. Zhu, W. Pan, X. Song, Y. Liu, X. Shao, Y. Tang, et al., The microRNA miR-23b suppresses IL-17-associated autoimmune inflammation by targeting TAB2, TAB3 and IKK-alpha, Nat. Med. 18 (2012) 1077–1086.
[37] C. Cao, Y. Zhang, Y. Chai, L. Wang, C. Yin, S. Shou, et al., Attenuation of sepsis-induced cardiomyopathy by regulation of MicroRNA-23b is mediated through targeting of MyD88-mediated NF-kappaB activation, Inflammation 42 (2019) 973–986.
[38] S. Lin, Q. Yin, Q. Zhong, F.L. Lv, Y. Zhou, J.Q. Li, et al., Heme activates TLR4-mediated inflammatory injury via MyD88/TRIF signaling pathway in intracerebral hemorrhage, J. Neuroinflammation 9 (2012) 46.
[39] X. Zhu, L. Tao, E. Tejima-Mandeville, J. Qiu, J. Park, K. Garber, et al., Plasmalemma permeability and necrotic cell death phenotypes after intracerebral hemorrhage in mice, Stroke 43 (2012) 524–531.
[40] E. Sekerdag, I. Solaroglu, Y. Gursoy-Ozdemir, Cell death mechanisms in stroke and novel molecular and cellular treatment options, Curr. Neuropharmacol. 16 (2018) 1396–1415.
[41] A. Chakraborty, S. Kim, S.H. Snyder, Inositol pyrophosphates as mammalian cell signals, Sci. Signal. 4 (2011) re1.
[42] E. Kim, J. Beon, S. Lee, S.J. Park, H. Ahn, M.G. Kim, et al., Inositol polyphosphate multikinase promotes Toll-like receptor-induced inflammation by stabilizing TRAF6, Sci. Adv. 3 (2017) e1602296.
[43] R. Xu, N. Sen, B.D. Paul, A.M. Snowman, F. Rao, M.S. Vandiver, et al., Inositol polyphosphate multikinase is a coactivator of p53-mediated transcription and cell death, Sci. Signal. 6 (2013) ra22.
[44] S. Bang, S. Kim, M.J. Dailey, Y. Chen, T.H. Moran, S.H. Snyder, et al., AMP-activated protein kinase is physiologically regulated by inositol polyphosphate multikinase, Proc. Natl. Acad. Sci. U. S. A. 109 (2012) 616–620.
[45] P. Guha, S.H. Snyder, Noncatalytic functions of IPMK are essential for activation of autophagy and liver regeneration, Autophagy 15 (2019) 1473–1474.
[46] B. Yuan, H. Shen, L. Lin, T. Su, L. Zhong, Z. Yang, Autophagy promotes microglia activation through Beclin-1-Atg5 pathway in intracerebral hemorrhage, Mol. Neurobiol. 54 (2017) 115–124.
[47] J. Harris, M. Hartman, C. Roche, S.G. Zeng, A. O'Shea, F.A. Sharp, et al., Autophagy controls IL-1beta secretion by targeting pro-IL-1beta for degradation, J. Biol. Chem. 286 (2011) 9587–9597.
[48] Y.T. Lin, H.C. Wang, H.C. Chuang, Y.C. Hsu, M.Y. Yang, C.Y. Chien, Pre-treatment with angiotensin-(1-7) inhibits tumor growth via autophagy by downregulating PI3K/Akt/mTOR signaling in human nasopharyngeal carcinoma xenografts, J. Mol. Med. 96 (2018) 1407–1418.
[49] X. Liu, Y. Deng, Y. Xu, W. Jin, H. Li, MicroRNA-223 protects neonatal rat cardiomyocytes and H9c2 cells from hypoxia-induced apoptosis and excessive autophagy via the Akt/mTOR pathway by targeting PARP-1, J. Mol. Cell. Cardiol. 118 (2018) 133–146.
[50] S.H. Baek, J.H. Ko, J.H. Lee, C. Kim, H. Lee, D. Nam, et al., Ginkgolic acid inhibits invasion and migration and TGF-beta-induced EMT of lung cancer cells through PI3K/Akt/mTOR inactivation, J. Cell. Physiol. 232 (2017) 346–354.
[51] N. Shinojima, T. Yokoyama, Y. Kondo, S. Kondo, Roles of the Akt/mTOR/p70S6K and ERK1/2 signaling pathways in curcumin-induced autophagy, Autophagy 3 (2007) 635–637.
[52] X. Li, C. Ren, S. Li, R. Han, J. Gao, Q. Huang, et al., Limb remote ischemic conditioning promotes myelination by upregulating PTEN/Akt/mTOR signaling activities after chronic cerebral hypoperfusion, Aging Dis. 8 (2017) 392–401.
[53] R. Zhang, Y. Zhu, X. Dong, B. Liu, N. Zhang, X. Wang, et al., Celastrol attenuates cadmium-induced neuronal apoptosis via inhibiting ca(2+)-CaMKII-dependent Akt/mTOR pathway, J. Cell. Physiol. 232 (2017) 2145–2157.
[54] Z. Yang, T. Zhao, Y. Zou, J.H. Zhang, H. Feng, Curcumin inhibits microglia inflammation and confers neuroprotection in intracerebral hemorrhage, Immunol. Lett. 160 (2014) 89–95.